

## GLOBAL JOURNAL OF ENGINEERING SCIENCE AND RESEARCHES

### EFFECT OF CHORD LENGTH OF A LOW SOLIDITY VANED DIFFUSER ON THE PERFORMANCE OF A CENTRIFUGAL COMPRESSOR STAGE

Venkateswara Rao Pothuri<sup>\*1</sup>, Venkata Ramana Murty G<sup>2</sup>, B. Amogh<sup>3</sup> & C. Pradeep Reddy<sup>4</sup>

<sup>\*1</sup>Associate Professor, Vasavi College of Engineering, India

<sup>2</sup>Professor, Vasavi College of Engineering, India

<sup>3,4</sup>Student, Department of Mechanical Engineering, Vasavi College of Engineering, India

#### ABSTRACT

CFD investigations are carried out on a low speed industrial centrifugal compressor stage to establish the comparison of performance with vaneless (VLD) and low solidity vaned diffuser (LSVD) and further to analyse the effect of chord length of the diffuser vane on the performance. The study is performed at an impeller speed of 4500 rpm, Mach number of 0.35 at impeller tip and at a setting angle of 24° at hub. In the present analysis, chord length is varied from 80 mm to 120 mm in steps of 10 mm at a given flow rate. Flow coefficient is varied from 80% to 120 % of design flow rate in steps of 10%, which includes the design and off design conditions. The overall stage performance is evaluated in terms of different performance parameters. From this study, it can be concluded that LSVD with 100mm chord length operating at design flow rate gives the best performance for the chosen configuration.

**Keywords:** *diffuser, impeller, chord length, flow rate, solidity.*

#### NOMENCLATURE

$C_p$  Static Pressure Recovery Coefficient,  
( $p_4 - p_2$ )/( $p_{02} - p_2$ )

$D$  Diameter (m)

$g$  Acceleration due to gravity ( $m/s^2$ )

$H$  Total head (m),  $\frac{\gamma}{\gamma-1} RT_{01} \left[ \left( \frac{P_{04}}{P_{01}} \right)^{\frac{\gamma-1}{\gamma}} - 1 \right] \frac{1}{g}$

$l$  Vane chord length (m)

LE Leading Edge

LSVD Low Solidity Vaned Diffuser

$m$  Mass flow rate (kg/s)

$n$  Speed (rpm)

$p$  Pressure (Pa)

$r$  Radius (m)

$R$  Gas constant (J/kgK)

$S$  Pitch (m),  $\pi D_3/Z$

$u$  Peripheral velocity (m/s),  $\pi D n / 60$

VLD Vaneless Diffuser

$Z$  Number of diffuser vanes

$\alpha$  Flow angle (deg)

$\beta$  Blade angle (deg)

$\eta$  Total-to-static stage efficiency (%),  $\left[ \frac{\left( \frac{P_4}{P_1} \right)^{\frac{\gamma}{\gamma-1}} - 1}{\left( \frac{T_{04}}{T_{01}} - 1 \right)} \right] * 100$

$\lambda$  Power coefficient,  $\phi\psi/\eta$

$\omega$	Angular velocity, rad/s
$\phi$	Flow coefficient, $m/(\rho u_2 \pi D_2^2/4)$
$\gamma$	Ratio of specific heats
$\rho$	Inlet density ( $\text{kg/m}^3$ )
$\sigma$	Solidity, $l/s$
$\psi$	Head coefficient, $H/(u_2^2/2g)$
CL*	Chord length of * mm
T*	Twist of * degree

## I. INTRODUCTION

Centrifugal compressors are a sub class of dynamic axisymmetric, work absorbing machinery. They are one of the old and most widely used turbomachinery in the industry. Even a small improvement in their performance would have a huge impact on the energy consumption. The main components of a centrifugal compressor are stationary casing, impeller, diffuser and return channel. Diffuser is a key component which contributes for the pressure rise desired. There are different configurations of the diffuser like vaneless diffuser, conventional vaned diffuser, low solidity vaned diffuser, partial vaned diffuser etc. Performance study of centrifugal compressor stage with vaneless and low solidity vaned diffuser using CFD software is presented in this paper.

## II. LITERATURE REVIEW

One of the main components of centrifugal compressors is diffuser, whose primary function is to convert kinetic energy of the fluids into static pressure. There are different types of diffusers, the simplest configuration being the “vaneless diffuser”. It is common practice by the centrifugal compressor manufacturers to produce compressors with large flow range for a variety of inlet conditions and process gases. Vaneless diffusers (VLD) have been the obvious choice for manufacturers due to many advantages like ability to accept wide range of inlet variations without any significant loss in performance; reasonable level of static pressure recovery; simple and cheap to manufacture; more tolerant to erosion and fouling; free from blade stalling and shock waves formation. However, VLD needs a large diameter ratio because of its low diffusion ratio. The constant angular momentum in free vortex leads to large sized diffuser having low energy conversion efficiency. Therefore, vaneless diffusers are suitable only for low pressure rise and are not suitable for aeronautical applications (Jonathan Everitt, 2010). Vaneless diffusers are mainly used in the process and refrigeration industries, and in automotive turbochargers.

The requirement for higher efficiency lead to the design of “vaned diffuser”. Even though the use of vaned diffuser improves pressure recovery, it reduces the operating range. In an attempt to overcome the deficiencies of the vaned diffusers, the concept of low solidity vaned diffuser (LSVD) was first developed by Senoo (1978) and later reported by Kaneki and Ohashi (1982), which has shown to have impressive efficiency gains than VLD with little or no loss in flow range. The primary feature of LSVD is the absence of geometrical throat between the vanes which improved the diffuser range both on the choke and stall side of the compressor. It is a good compromise between vaneless and vaned diffusers, which has better pressure recovery than the former and wider flow range than the latter.

Osborne and Sorokes (1988) have shown that with LSVD, efficiency and head were improved at design and low flow conditions relative to that of vaneless diffusers. The design of LSVD is based on “classical vane diffuser theory”. Kmecl et al. (1999) showed that the blade thickness distribution and shape of profile had minor effect on the diffuser profile losses. In general, it can be seen that an aerofoil shape results in slightly better performance than a simple flat plate diffuser even though the effect is small. One of the reasons for this is the sensitivity of a flat plate to incidence as observed by Engeda (2001). The effect of incidence seems to be important for LSVD performance and a small negative incidence is found to be beneficial for performance and operating map. The work of Hohlweg et al. (1993) indicated that positive incidence should be avoided. Hayami et al. (1989) showed that the LSVD had maximum pressure recovery at an incidence angle of  $-2^\circ$  to  $-3^\circ$ . Siva Reddy et al. (2004) stated that an aerofoil

shaped diffuser has the ability to handle positive and negative incidences. Numerical results of Turunen- Saaresti (2004) predicted that a circular arc camber line diffuser with NACA 65-10 profile results in the highest efficiency at the design point when compared with constant thickness flat plate and circular arc designs.

The effect of Radial gap between rotor and diffuser is studied in terms of radius ratio. Anish and Sitaram (2009) showed that the pressure rise coefficient of diffuser shows the best overall characteristics when the gap is 1.05 and suggested that at design and low flow coefficients, the narrowest radial gap is the best configuration at high flow coefficient while at low flow coefficients, it produces lowest stage efficiency. Higher operating range and peak energy coefficient can be observed when the diffuser vane leading edge is kept far away from the impeller. Hayami et al. (1989) showed the LSVD with 0.69 solidity performed better than the vaneless diffuser of a transonic centrifugal compressor. From the literature, it is recommended that a solidity close to 0.75 should be used for the initial design. Study of Oh and Agarwal (2007) on the effect of solidity on high pressure ratio compressor revealed that the optimum solidity for their application is 0.71 in terms of operating range and better performance. Engeda (2003) concluded that the vane turning angle is also the major parameter affecting the performance and found that higher turning angle produces higher diffuser pressure recovery at high mass flow rates due to lower losses and blockage at stall on the pressure surface of vanes. He showed that most of the pressure is recovered by the vaneless part at high flow, which indicates the importance of having a vaneless part after the vanes.

A significant amount of research has been dedicated to study the impeller exit flows, impeller with vaneless diffuser, conventional vaned diffuser and low solidity vaned diffuser. The purpose of the current numerical investigation is to assess the effect of chord length on the performance of the centrifugal compressor stage.

### III. COMPRESSOR DETAILS

The details of the centrifugal compressor used for the present analysis are as specified in Table 1. The analysis is done at five different flow coefficients, at 80%, 90%, 100%, 110% and 120% of design flow rate by varying the chord length from 80 mm – 120 mm in steps of 10mm representing the design and off design cases for vaneless and twisted vaned diffusers. The impeller details are taken from Siva Reddy et al. (2007). The diffuser passage length is extended by 25mm to facilitate the analysis with longer chord lengths.

*Table 1. Details of the compressor*

Speed, n	4500 rpm
Impeller vane radius at inlet	150 mm
Impeller vane outlet at radius	250 mm
Diffuser vane radius at inlet	275 mm
Diffuser vane radius at outlet	377 mm
Impeller width	24.5 mm
Blade angle at impeller inlet, $\beta_1$ w.r.t. tangential direction	27°
Blade angle at impeller exit, $\beta_2$ w.r.t. tangential direction	45°
Width of the diffuser passage, b	24.5 mm
Mass flow rate, $\dot{m}$	1.3 kg/s
Diffuser blade chord length at hub, l	80 mm -120mm
Number of impeller blades	17
Number of diffuser blades, Z	14

### IV. DETAILS OF THE NUMERICAL MODEL AND MESHING

CFD simulations are performed on a single impeller and diffuser passage by applying periodic boundary condition, since the geometry of impeller and diffuser are cyclic symmetric. This avoids the necessity of modelling the entire centrifugal compressor stage, thereby saving enormous computational time and resources. Impeller is a rotating domain and diffuser is the stationary one. For numerical simulation, a three dimensional domain is modelled, as

flow is fully three dimensional inside the domain. Vaneless diffuser is modelled and discretized using GAMBIT software. The geometry of Impeller and Low solidity vaned diffuser is modelled using commercial software. For the analysis, the diffuser passage length is extended by 25mm to avoid the back pressure.

For the Impeller and Low solidity vaned diffuser, meshes are generated using ANSYS-TurboGrid. B-Spline curve is used for generating hub, shroud and blade profiles. For impeller the trailing edge definition is given as cut-off or square, so that the outlet gets aligned with the trailing edge. This option is intended for use on blade profiles that have discontinuities in slopes at the edges and to produce a flat leading/trailing edge between two edge curves. The method used in the topology is traditional with control points. The topology definition defines the way in which the mesh is generated. Then 3D mesh is generated with structured hexahedral grids. All the meshes are generated with face angle ranging between  $15^\circ - 165^\circ$ . Grid independence studies are conducted at design flow conditions where for a chosen configuration, four grids are generated with the number of elements varying from 75000-150000 in steps of 25000. To improve the mesh quality, C-grid and O-grid topologies are incorporated. Static pressure recovery coefficient formed the basis for selecting the best mesh size. After carrying out pre-processing, solving and post-processing with all the meshes, best mesh with regards to static pressure recovery coefficient is selected and with the best mesh, further analysis is carried out by varying the flow rates at design and off-design cases.

## V. BOUNDARY CONDITIONS AND METHODOLOGY

All the simulations are carried out using ANSYS-CFX. The type of simulation chosen is Turbomachinery and steady state analysis is performed. In order to ensure that the boundary conditions are not affected by the back pressure, the inlet of the computational domain is kept ahead of the eye of the impeller. The wall configuration is specified as no tip clearance at hub, shroud and diffuser. For the present analysis, fluid used is air and is assumed as ideal gas. Air enters axially at inlet. The reference absolute pressure used is 95000 Pa. The direction of flow is specified as normal to boundary. Mass flow rate is specified as outlet condition with mass flow per passage equal to 0.07467 kg/s for the compressor stage with vaneless diffuser and 0.0928 kg/s with low solidity vaned diffuser. For the side walls of impeller and diffuser, rotational periodic boundary condition is specified. Total energy model is the heat transfer model employed for temperature calculations. The turbulence model used is standard k- $\epsilon$  model and the turbulence intensity is selected as 0.05 and Eddy length scale as 0.03 m, which is in line with the computations carried out by Tarek Meakhail and Seung O Park (2004) on a centrifugal fan. The wall influence on flow of the shroud wall of the impeller domain is specified as counter rotating type, Stage-mixing plane interface is used in between the outlet of the impeller and inlet to the diffuser. This model allows steady state predictions to be obtained for multi-stage machines. For the calculation of advection terms, a high resolution scheme is used.

The governing equations used for simulations are the Reynolds-averaged continuity equation, the momentum equation, and the energy equation. For discretizing the governing equations, Finite volume approach is used which ensures conservation of mass, momentum and energy over any region of computational domain. For steady state problems, the time step behaves like an acceleration parameter to guide the approximate solutions in a physically based manner. This reduces the number of iterations required for convergence. The fluid time step is given as  $0.1/\omega$  where  $\omega$  is the angular velocity in rad/s. The convergence of RMS residuals for all the equations is resolved to  $1 \times 10^{-5}$ . Post processing of data was carried out resulting in fringe plots for better understanding of fluid flow through the chosen centrifugal compressor stage. Session files are recorded with all necessary outputs taken in required sequence and is loaded with the extension .cse as a template to CFD-Post., as similar plots and figures are desired for all the cases A batch file with the necessary commands to generate the reports is executed with the recorded session file given as an argument to the command. From these generated reports, required parameters for the calculation of flow parameters are extracted using a python code. Then the flow parameters are calculated for all the configurations under study and the desired plots are generated.

**VI. RESULTS AND DISCUSSION**

The following figures show the variation of normalized flow properties and static pressure recovery coefficient with normalized flow coefficient for different configurations of LSVD. Normalization has been carried out with reference to the data of VLD at design flow conditions.

**Total-to-static stage efficiency**

Centrifugal compressor stage performance is evaluated by means of stage efficiency. It is evaluated based on the conditions at the impeller domain inlet and diffuser domain outlet. Hence, this gives the measure of combined performance of the impeller and diffuser. Figure 1 shows the variation of normalized total to static stage efficiency of VLD and LSVD with different chord lengths for different flow coefficients. It can be observed that the total to static stage efficiency increased as the diffuser configuration changes from VLD to LSVD. This is due to the retardation of flow caused by the introduction of vane. There is an increase in efficiency with the increase in mass flow rate up to the design flow rate and decreased thereafter. With respect to chord length there is an increase in efficiency from chord length 80mm to 100mm and decreased thereafter. This may due to the increased skin friction drag due to increase in chord length of the vane.

**Static pressure recovery coefficient**

The kinetic energy leaving the impeller tip is converted to the static pressure rise as the flow passes through the increasing area of diffuser passage. Static pressure recovery coefficient ( $C_p$ ) describes the amount of static pressure recovered from the available dynamic head at the diffuser inlet. From figure 2, it can be observed that there is an increase in static pressure recovery coefficient as the diffuser configuration changes from VLD to LSVD, due to the retardation of flow with the introduction of vane. It increased with the increase in mass flow rate up to design flow rate and then decreased. The reason for this can be attributed to the higher drag caused by the longer chord lengths 110mm, 120mm.

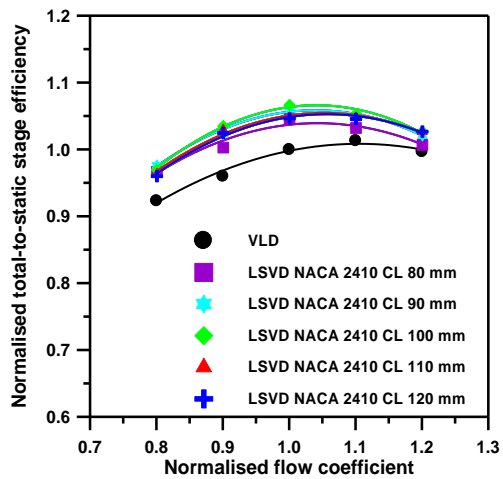


Fig.1 Variation of normalized total to static stage efficiency at various flow rates

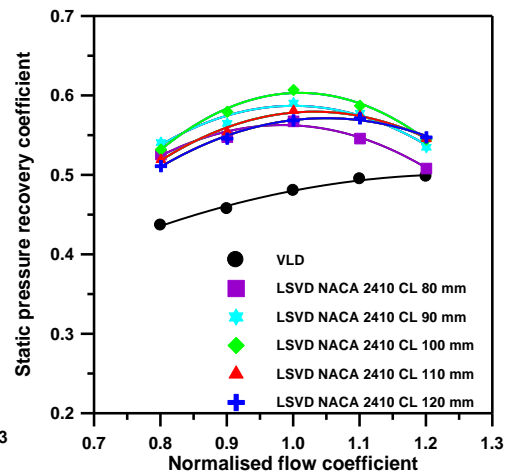


Fig.2 Variation of Static pressure recovery coefficient at various flow rates

**Static head coefficient**

Static head describes the amount of static pressure rise from impeller inlet to the diffuser outlet. From figure 3, it can be observed that there is an increase in static head coefficient as the diffuser configuration changes from VLD to LSVD. It has decreased with the increase in mass flow rate up to design flow rate. With the increase in mass flow rate, the velocities alter, incidence angle increases and thus incidence losses occur, due to which the static pressure rise drops.

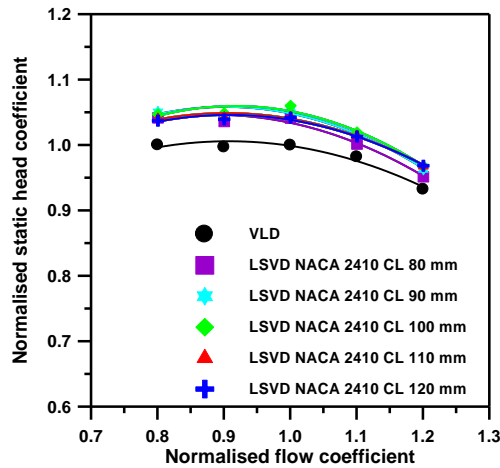


Fig. 3 Variation of Normalized static head coefficient at various flow rates

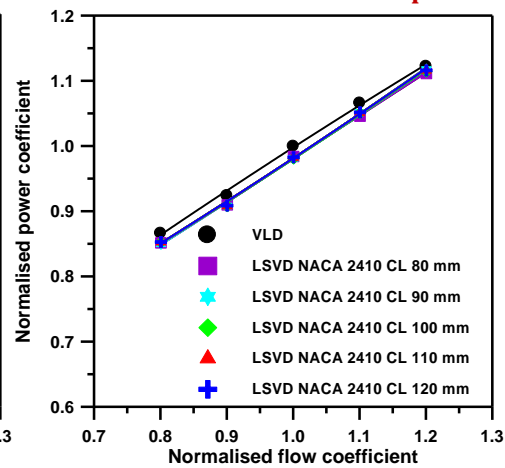


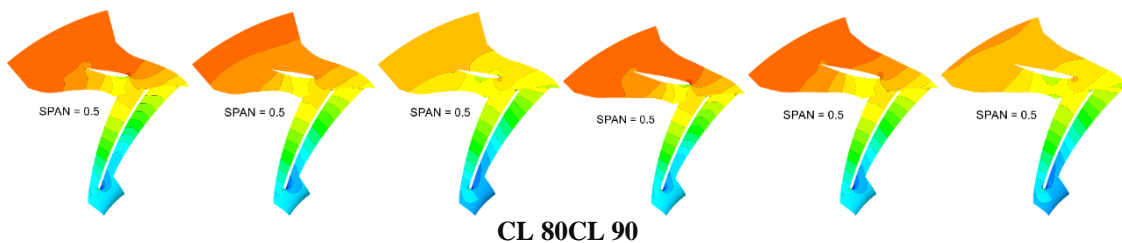
Fig.4 Variation of Normalized power coefficient at various flow rates

**Power coefficient (LSVD)**

The value of power coefficient provides information about the energy required by the fluid as it passes through the impeller and diffuser. Irrespective of type of diffuser, with the increase in mass flow rate power consumed increases implying power coefficient increases. From Fig.4, it can be observed that the normalized power coefficient has decreased as the diffuser configuration changes from VLD to LSVD, due to the introduction of vane by which the static head increases. It has increased gradually with the increase in mass flow rate and is least for LSVD with chord length 80mm at flow coefficient of 0.8. But its effect is negligible on the performance of compressor with LSVD. From figure 6, it can also be concluded that the variation in power coefficient follows the general trend of the normal limiting characteristic for a backward curved bladed impeller.

**Variation of absolute pressure in the stage**

Figure 5 shows the variation of normalized absolute pressure for LSVD from the inlet of the compressor to the exit of it at mid-span along the stream wise direction. The absolute pressure coefficient is obtained by normalizing the local total pressure with the absolute pressure at the impeller exit,  $(95000 + 0.5\rho_2u_2^2)$ . Variation is shown for 80%, 100%, 120% of the design mass flow rate for all the chord lengths considered in the present analysis. As the fluid advances from the inlet to the exit of the compressor, pressure gradually increases for all mass flow rates, which is the basic purpose of any compressor. Increase in pressure is more at low flow coefficients compared to the high flow coefficients. But maximum pressure rise is observed at design flow coefficient for all the chord lengths considered. As the chord length increases, pressure rise increases up to 100mm chord length and decreases thereafter, which is due to the increased drag offered by longer chord lengths.





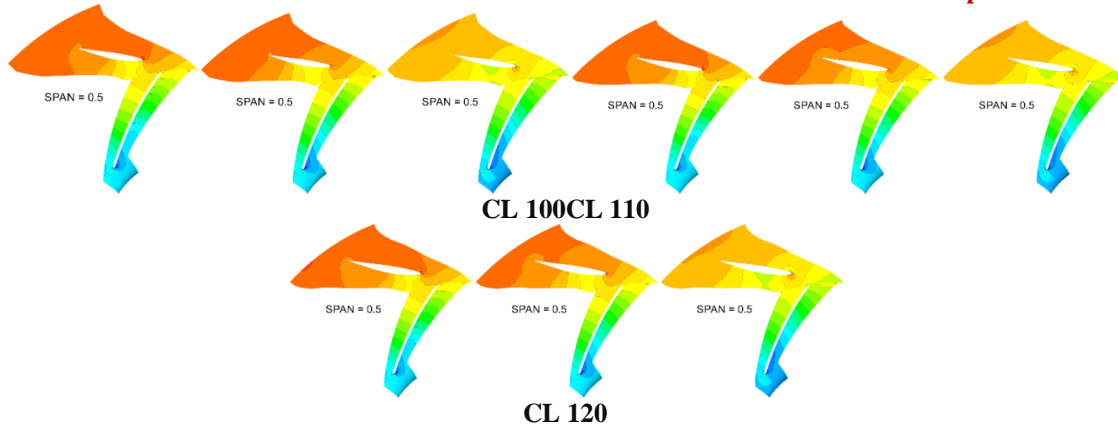


Fig.5 Variation of Normalized absolute pressure for LSVD at 80 %, 100% and 120 % of design flow rate

**Flow Analysis inside Impeller**

**Relative total pressure**

Figure 6 shows the relative total pressure on the suction surface (SS) and pressure surface (PS) of the impeller blade at design flow coefficient. These contours are shown for the impeller with LSVD at downstream at 100 mm chord length. Relative total pressure represents the flow behavior inside a rotor correctly, as it is calculated by adding the static pressure to the dynamic head based on the relative velocity. As the flow turns from axial to radial direction, there is pressure gradient from hub to tip. This gradient decreases in the streamwise direction and becomes uniform at exit. Low relative total pressure is observed on the suction side near the axial to radial bend. Similar variations are observed for the impeller with LSVD at downstream.

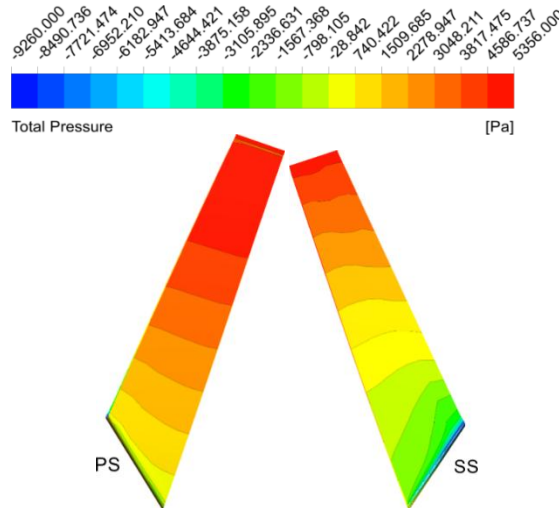


Fig.6 Variation of Relative total pressure at suction and pressure sides of the impeller blades

**Meridional Velocity Variation**

In this section flow behavior inside the impeller is analyzed with different types of diffusers in the downstream. The impeller remains same for all diffuser configurations and the flow field inside the impeller remains same. There is no change in the leading edge of the diffuser blade. Figures 7(a) and 7(b) show the normalized meridional velocity variation in the impeller at different sections in the streamwise direction at design flow coefficient. These contours are shown for the impeller with VLD and LSVD with 100 mm chord length, downstream. Normalization is done

with impeller tip peripheral velocity. These contours suggest that irrespective of the type of diffuser at downstream, the meridional velocity inside the impeller domain remains unaltered.

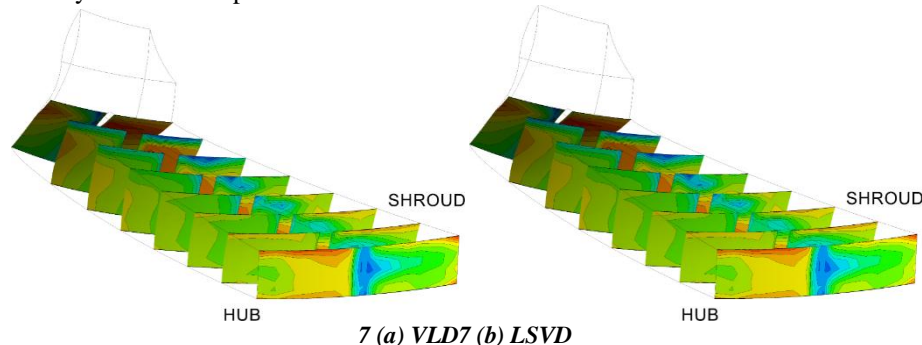


Fig.7 (a) and (b) Variation of normalized meridional velocity in the impeller

## VII. CONCLUSIONS

CFD investigations are conducted to analyse and compare the performance of the compressor stage with vaneless and low solidity vaned diffusers and in turn to establish the effect of chord length of diffuser vane at impeller speed of 4500 rpm and at a setting angle of  $24^\circ$  at hub. Analysis was carried out at five different chord lengths (80mm, 90mm, 100mm, 110mm, 120mm) at design flow rate (1.3kg/s) and off-design flow rates (80%, 90%, 110% and 120% of the design flow rate). From the analysis, it can be concluded that with respect to flow parameters stage efficiency, static pressure recovery coefficient, static head coefficient, power coefficient the performance of centrifugal compressor stage improved with LSVD for all configurations. Among the different configurations of LSVD considered for the analysis, the best one is with chord length 100mm, at design flow rate (1.3 kg/s) which is bolstered by the following numbers. Relative to the data of VLD at design flow conditions, maximum increase of the normalized total to static stage efficiency is 6.69%; maximum increase of static pressure recovery coefficient is 12.69%; maximum increase of normalized static head coefficient is 6.05% for LSVD with 100mm chord length at design flow rate. The performance of the impeller was not influenced by the shape and chord length of the diffuser vane in the downstream.

## REFERENCES

1. **Abraham Engeda** "The Design and Performance Results of Simple Flat Plate Low Solidity Vaned Diffusers", 2001.
2. **Abraham Engeda** "Experimental and Numerical Investigation Performance of A 240kw Centrifugal Compressor with Different Diffusers" *Experimental Thermal and Fluid Science* 28 55-72, 2003.
3. **Amineni, N. K., Engeda, A., Hohlweg, W. C. and Direnzi, G. L.** (1996) "Performance of Low Solidity and Conventional Diffuser Systems for Centrifugal Compressors". *ASME Paper 96-GT-155*.
4. **Anish S, Sitaram N:** "Computational Investigation of Impeller-Diffuser Interaction in A Centrifugal Compressor with Different Types of Diffusers" *Proceedings of The Institution of Mechanical Engineers, Part A: Journal of Power and Energy* 2009 223: 167 Doi: 10.1243/09576509jpe662.
5. **Hayami, H., Senoo, Y. and Utsunomiya, K.** (1989) "Application of Low-Solidity Cascade Diffuser to Transonic Centrifugal Compressor". *ASME Paper 89-GT-66*.
6. **Jonathan Everitt** "Investigation of Stall Inception in Centrifugal Compressors Using Isolated Diffuser Simulations" M.S thesis, Department of Aeronautics and Astronautics on August 20, 2010
7. **Kaneki, T. and Ohashi, S.** (1982), "High efficiency multistage centrifugal compressor". *Hitachi Rev.*, 1982, 31(6), 287-291.
8. **Knecl, T., ter Harkel, R. and Dalbert, P.** (1999) "Optimization of a Vaned Diffuser Geometry for Radial Compressor, Part II: Optimization of a Diffuser Vane Profile in Low Solidity Diffusers". *ASME Paper 99-GT-434*.
9. **Nakagawa, K., Hayami, H., and Keimi, Y.** (2003) "Comparison of two diffusers in a transonic centrifugal compressor". *International J. Rotating Machinery*. 9, 279-284.



10. **Oh, J., C.W. Buckley, and G.L. Agrawal**, “Numerical Investigation of Low solidity vaned diffuser performance in a High-Pressure Centrifugal Compressor: Part II-Influence of Vane Stagger” Paper no. GT2008-50178, 1487-1494, 2008.
11. **Osborne, C., and Sorokes, J. M.**, “The Application of Low Solidity Diffusers in Centrifugal Compressors” *Flows in Non-Rotating Turbomachinery Components*, ASME Fedvol, 1988.
12. **Senoo, Y.**, Japanese Patent Application Disclosure 119411 / 78, October, 1978.
13. **Siva Reddy, T. Ch., Ramana Murty, G. V., Mukkavilli, P., and Reddy, D. N.** “Effect of the setting angle of a low-solidity vaned diffuser on the performance of a centrifugal compressor stage”. *Proc. Instn Mech. Engrs, Part A: J. Power and Energy*, 2004, 218, 637– 646.
14. **Siva Reddy, T.Ch.**, (2007), “Flow investigations on Low Solidity Vaned Diffusers of a centrifugal compressor stage”, PhD Thesis, Department of Mechanical Engineering, Osmania University, Hyderabad, India.
15. **Turunen-Saaresti, T.** (2004) “Computational and Experimental Analysis of Flow Field in the Diffusers of Centrifugal Compressors”. *Acta Universitatis Lappeenrantaensis* 192, dissertation, Lappeenranta University of Technology, Finland.
16. **William C. Hohlweg, Gregory L. Direnzi, Ronald H. Aungier.**, “Comparison Of Conventional And Low Solidity Vaned Diffusers” ASME 1993 International Gas Turbine and Aeroengine Congress and Exposition, Volume 1: Aircraft Engine; Marine; Turbomachinery; Microturbines and Small Turbomachinery, Cincinnati, Ohio, USA, May 24–27, 1993, ISBN: 978-0-7918-7888-0.